Surface Review and Letters, Vol. 6, No. 1 (1999) 45–52

SILICON OXIDE DECOMPOSITION AND DESORPTION DURING THE THERMAL OXIDATION OF SILICON

D. STARODUB, E. P. GUSEV, E. GARFUNKEL and T. GUSTAFSSON
Departments of Chemistry and Physics, and Laboratory for Surface Modification, Rutgers University, Piscataway, NJ 08854-8087, USA

Received 1 July 1998

The thermal oxidation of silicon is normally considered to occur via two different routes. At higher O_2 pressures and lower temperature SiO_2(s) film growth occurs ("passive" oxidation), while at lower O_2 pressures and higher temperature SiO(g) is desorbed in an etching process ("active" oxidation). We have measured the yield of SiO into the gas phase in a wide range of dry O_2 pressures (10^{-7}–10^{-5} Torr) and Si substrate temperatures (620–870°C) in the passive as well as the active oxidation regimes. A phase diagram for silicon oxidation in this pressure–temperature region is obtained. We have found evidence for small but measurable yields of SiO(g) desorbing from the nascent oxide film during the initial stages of passive oxidation, even when the oxide film continuously covers the surface. A sensitive method for detecting volatile products based on condensation of desorbed species is described.

1. Introduction

The phase diagram in pressure–temperature (P–T) coordinates for thermal oxidation of both Si(100) and Si(111) in dry O_2 has been investigated by many groups.[1–7] It consists of two main regions, separated from each other by a transition region in the vicinity of a line given by the expression $P(T) = P_0 \times \exp(-\Delta E/kT)$, where $P_0 \cong 2 \times 10^{12}$ Torr and $\Delta E \cong 3.8$ eV for both Si(100) and Si(111) to within experimental error.[3]

At low temperatures and high oxygen pressures "passive" oxidation takes place, and an amorphous silicon dioxide film grows on the substrate following the net reaction $2Si(s) + O_2(g) \rightarrow SiO_2(s)$. This process is crucial for applications in the semiconductor industry, and has attracted considerable attention from researchers for many years.[8–20] The growth of thick (> 200 Å) oxide films is usually described by the classical Deal–Grove (DG) model.[9] In this model the limiting stages for oxidation are either (i) reaction between oxygen and silicon at the silicon/oxide interface for thinner films (with an initial linear oxide thickness vs. time dependence), or (ii) diffusion of molecular oxygen through the oxide film to the reaction sites at the interface for thicker films [a parabolic dependence of oxide film thickness (x) with time (t) $x^2 \sim t$]. However, the DG model fails to account for a faster-than-predicted rate of growth for thin films (< 200 Å). Several mechanisms have been proposed to explain this anomaly.[21] They include the "blocking layer" model,[22] the "fast initial growth" model,[12] the "reactive" layer model,[13,17] the "parallel oxidation" model,[14,18] and other modifications of the basic DG model. No satisfactory experimental confirmation of these models exists (although some have been proven wrong), and the oxidation mechanism for ultrathin silicon oxide films remains incompletely understood.[23]

At high substrate temperatures and low oxygen pressures, the net reaction $2Si(s) + O_2(g) \rightarrow 2SiO(g)$ occurs, resulting in desorption of SiO. This regime is referred to as "active" oxidation, and under these conditions the silicon surface remains free of oxide. The active oxidation reaction has been studied, for example, using modulated molecular beam reactive scattering (MMBRS).[15,19,24] The formation of volatile SiO can also take place as a result of high temperature SiO_2/Si decomposition via the apparent reaction $Si(s) + SiO_2(s) \rightarrow 2SiO(g)$ when the oxygen partial pressure is low. In the presence of gaseous oxygen, the reoxidation reaction $2SiO(g)$ [or $2SiO(surface)$] $+ O_2(g) \rightarrow 2SiO_2(s)$

is also possible. Silicon oxide decomposition can be used to help obtain a clean silicon surface.[25] The decomposition reaction, however, can also have a detrimental role during postoxidation annealing of SiO_2 films (in nitrogen, vacuum, etc.), because it can lead to the formation of microvoids in the oxide films, which in turn results in deterioration of their electrical properties.[26,27] Investigations of Si oxide decomposition[15,19,24–26,28–34] have covered a range from the oxygen coverage of 0.003 ML[35] to oxide films of $>$ 500 Å thickness[29] and temperatures of 900–1200 K. A variety of methods have been used for monitoring changes in the film, including scanning tunneling microscopy (STM)[31,34] and atomic force microscopy (AFM),[36] X-ray photoelectron spectroscopy (XPS),[32] scanning Auger (SAM) and electron (SEM) microscopy,[28–30,32] medium energy ion scattering (MEIS)[28] and optical second-harmonic generation (SHG).[37] Gaseous products of oxide decomposition have been studied using temperature-programmed desorption (TPD) measurements.[15,19,24,31] It was shown that film decomposition is an inhomogeneous process occurring via void formation, with the voids nucleating at the SiO_2/Si interface.[28,32] The voids spread through the film, eventually exposing the clean Si surface. They then expand laterally as the remaining SiO_2 is consumed at the Si/SiO_2 interface, with no detectable thinning of the rest of the film. TPD studies demonstrate a strong dependence of desorption temperature on both film thickness[24] and chemical treatment of the Si substrate[33] caused by variations in the interface chemical bonding.

A transition regime is now thought to exist between the active and passive regions of the P–T phase diagram.[5,6,38] Oxidation in the transition regime results in the development of a rough surface.[39] Our recent MEIS study[40] has shown that some oxygen is present on the surface under these conditions in the form of passive oxide islands; concurrently, Si etching takes place on the oxygen-free part of the Si surface.[5,6,38–40] The inhomogeneous etching results in significant roughening. We should note that the transition region may have a somewhat broad temperature range, at least at low pressures. For example, the transition region was estimated[40] to be about 50 K wide at 10^{-6} Torr. An additional complication is that the existence and position of the transition region are influenced by the initial conditions (i.e. pre-existing oxide). In microelectronics technology, the transition regime with SiO etching and SiO_2 oxide film growth competing may accidentally arise during high temperature Si annealing in "nominally" inert ambient gases (N_2, Ar, etc.) with very small partial pressures of residual O_2.[41]

Usually, the reactions to form SiO_2(s) (passive oxidation) and SiO(g) (active oxidation and SiO_2 decomposition) are considered separately, with the exception of the transition regime and the first monolayer stage of passive oxidation where these reactions are competitive. This is seemingly reasonable, given that they each occur in a different part of P–T phase space. Nevertheless, some models of Si passive oxidation[42] suggest that the gaseous SiO forms on "special" sites (possibly defects) at the interface in parallel with SiO_2 (formed in the dominant reaction pathway), and that the SiO formed can outdiffuse through the oxide film. In these models, the reactions of SiO_2 and SiO formation are considered as competing with each other. Recently, Takakuwa *et al.*[43,44] further suggested that decomposition of SiO_2 near the interface occurs simultaneously with SiO_2 formation and oxidation of out-diffusing SiO (the volatile product of SiO_2 decomposition), and that this might also be an important channel for silicon oxide film growth. The most straightforward evidence for the importance of the decomposition reaction and/or gaseous SiO species formation during passive oxidation should be provided by a direct observation of SiO escaping into the gas phase. But the transport of SiO into the gas phase has been measured only during active oxidation and oxide film decomposition in vacuum.

In this paper we present the results of measurements of the rate of SiO transport into the gas phase for the passive Si oxidation regime. Because the rate of SiO desorption is expected to be very low,[45] we have measured the *total* yield of SiO into the gas phase. For this purpose, a metal foil was placed in front of the Si sample, such that the Si that leaves the surface during oxidation (in the form of SiO) was trapped on the foil. The amount of silicon and oxygen deposited on the metal foil was directly measured by XPS.

2. Experimental

Experiments were carried out *in situ* in a UHV chamber with a base pressure in the 10^{-11} Torr range.

The chamber was equipped with an XPS system and a quadrupole mass spectrometer for monitoring surface and gas composition, respectively. A low energy sputter gun was used for cleaning the foil between experiments. In XPS, we used the Al K_α line (photon energy 1486.6 eV). Silicon (35 mm × 7 mm) samples were cut from Si(100) n-type (resistivity 20 Ω·cm) wafers covered by a 20 Å protective oxide. The Si slabs were clamped in molybdenum clips. In order to avoid metal contamination of the Si surface from the sample holder due to diffusion at high temperatures, Si pads were inserted between the sample and the molybdenum clips. The sample was heated by direct current to temperatures of 600–1100°C. An optical infrared pyrometer and a thermocouple were used to measure the sample temperature. Sample heating was uniform along most of the sample and dropped by 10–30°C in narrow regions near the clips.

The Si sample was cleaned in dehydrated ethanol and rinsed in distilled water. After loading into the chamber, it was degassed at temperatures of 700–780°C for ∼ 24 h and flashed several times to 1000–1100°C to obtain a clean surface. Research grade 99.998% oxygen was introduced through a leak valve into the chamber, which was pumped continuously with a turbomolecular pump. The metal foil was mounted on a manipulator with LN_2 cooling. It could be placed in front of the silicon sample during thermal oxidation and repositioned for the XPS measurements and cleaning by Ar ion sputtering. The temperature of the foil could be varied in the range of 100–400 K by LN_2 cooling and heating by a filament from the back of the foil; the foil temperature was measured with a thermocouple. The material for the foil was chosen such that: (a) it should not be readily oxidized by O_2 under our experimental conditions (pressures in the range of 10^{-7}–10^{-5} Torr and foil temperature of 100–300 K), and (b) it should not have XPS peaks which could mask the O 1s and Si 2p or/and 2s peaks. Although Au and Pt are obvious choices for a substance which does not react in vacuum with O_2, Ag was chosen because of less XPS peak overlap. The Si 2p peak is partially masked by the low energy tail of the Ag 4s peak (97 eV), but the Si 2s peak is well separated from any Ag peaks. We found that the slight oxidation of the Ag foil did not influence the amount of Si deposited on it. After cleaning the Ag foil by Ar^+ ion bombardment, no XPS intensity from silicon, oxygen or carbon could be detected.

To find out the fraction of the SiO flux leaving the Si sample that can be trapped on the Ag foil, calibration experiments were performed. We used the fact[15] that at room temperature the oxygen coverage is saturated at 1.0 ML [6.8×10^{14} cm^{-2} for Si(100)] for O_2 exposures more than approximately 700–800 L. After a silicon sample, pre-exposed to O_2 at pressure 10^{-6} Torr for 15 min (exposure 900 L), is heated to 800–900°C, it can then be expected that about 1 ML of Si will be transported to the gas phase in the form of SiO species. The area of the Si 2s photoelectron peak from Si captured by the Ag foil should correspond to $\sim 6.8 \times 10^{14}$ cm^{-2} of Si atoms, assuming a sticking coefficient of ~ 1 and neglecting geometrical factors. The Si coverage on the Ag foil was also evaluated independently by comparing the areas of the Si 2s and Ag $3d_{5/2}$ peaks and using known atomic sensitivity factors[46] (0.29 for Si 2s and 3.1 for Ag $3d_{5/2}$, relative to F 1s = 1) and escape lengths for photoelectrons[47] (36 Å for Si 2s photoelectrons in a SiO_2 matrix). The Si coverage calculated this way was found to be $\sim 5.5 \times 10^{14}$ cm^{-2}. Since the results agree to within 20%, we argue that most of the Si leaving the Si sample can be trapped by the foil as anticipated. For most cases, the area under the Si 2s peak was assumed to be proportional to the amount of SiO that escaped from the Si sample, for two reasons: (a) except for oxidation in the active regime, the amount of Si on the foil never exceeded 2–3 ML, so the attenuation of the photoelectron yield due to their limited inelastic mean free path is small, and (b) the area under the Si 2s peak is proportional to the number of subsequent deposition experiments performed without cleaning the Ag foil, which means that there is no noticeable dependence of the SiO sticking coefficient on the silicon and oxygen coverage of the foil. Our measurements have also shown that the presence of the metal foil does not influence the oxidation conditions on the Si sample, except for an additional heating of the Si sample by about 15°C (at 700°C) because of the reflected radiation. The fraction of desorbed Si that is trapped by the metal foil depends only on the distance between the Si and Ag plates. Note that the equilibrium silicon pressure never exceeded 3×10^{-10} Torr for the temperatures used in our experiments[48] ($< 1.4 \times 10^{-12}$ Torr for the temperature of 730°C, which corresponds to a

flux of $< 5 \times 10^{-7}$ ML/s), and so the evaporation of pure Si can be considered negligible. This was confirmed experimentally by heating the clean Si sample in front of the Ag foil in vacuum. No Si 2s signal was observed after this procedure.

Though the method we present cannot compete in terms of time resolution with measurements of gaseous SiO employing a mass spectrometer (MS) in MMBRS[19] (better than 0.1 ms) or laser-induced fluorescence (LIF) techniques[45] ($\sim$ 0.1 s), we believe that under certain circumstances our method can be very useful because it allows one to accurately measure the *integrated* amount of gaseous decomposition products and the *mean* rate of SiO transport into the gas phase for low rates of SiO_2 decomposition (and/or direct SiO desorption). Furthermore, our method can be applied to measurements during passive oxidation where any direct observation of SiO desorption (from SiO_2 decomposition) during film growth would be notable, as it has so far never been observed. At very low SiO desorption rates, the monitoring of gas phase species fails due to a lack of sensitivity. Integration methods can also be used with the LIF or MS techniques; however, it is not clear that the signal/noise improvement will be sufficient. In our arrangement, noise appears only as noise in the integrated XPS spectra. The sensitivity can be increased further by using longer data accumulation times or by repeating the same oxidation procedure several times and cleaning the Si surface between cycles.

To estimate the sensitivity of our method, one should note that about 0.1 ML Si coverage on Ag can be detected by XPS. This means that for an oxidation experiment which lasts, for example, for 5 h, a sensitivity of about 5×10^{-6} ML/s for the *mean* SiO desorption rate can be achieved (we are clearly measuring an integrated, not instantaneous, rate). This is 1–2 orders of magnitude higher than for LIF, which is reported[45] to be 10^{-4}–10^{-5} ML/s. Moreover, unlike LIF and MS, methods such as ours based on trapping of the desorption product can be expanded to higher oxygen pressures such as those that occur under realistic device processing conditions, although additional calibration would probably be needed to account for viscous gas flow between the Si and Ag plates (i.e. when the molecular mean free path becomes much shorter than the distance between the plates). Finally, we note that temperature uniformity and geometrical issues must be carefully addressed in all methods.

3. Results and Discussion

We measured the amount of SiO leaving the Si sample in both the passive and active oxidation regimes. The experiments were performed at O_2 pressures of 10^{-7}–10^{-5} Torr over a range of temperatures 620–870°C for oxidation times of 2–20 min. A typical set of spectra taken in the Si 2s peak region (for SiO_x/Ag) after the first 10 min of oxidation at a fixed pressure and different temperatures is shown in Fig. 1. The main concern in our measurements was peak intensities, and we note that the shifts in the binding energies clearly seen in these spectra may be due to state changes with increasing coverage. The dependence of the integrated area under the Si 2s peak (which is proportional to the total SiO yield)

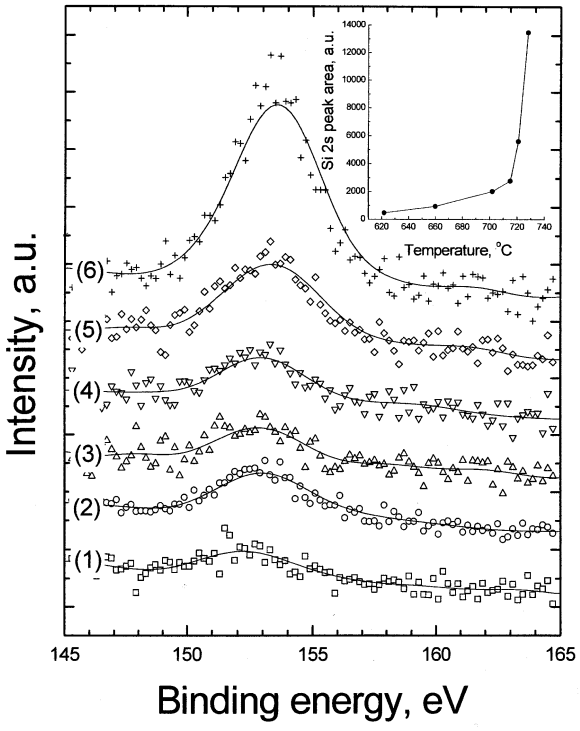

Fig. 1. Si 2s spectra for silicon deposited on Ag during the first 10 min of oxidation at pressure of 10^{-7} Torr and different temperatures: (1) 620°C (3 cycles), (2) 660°C (3 cycles), (3) 700°C, (4) 715°C, (5) 720°C, (6) 728°C. *Inset*: temperature dependence of the area under the Si 2s peak for a pressure of 10^{-7} Torr.

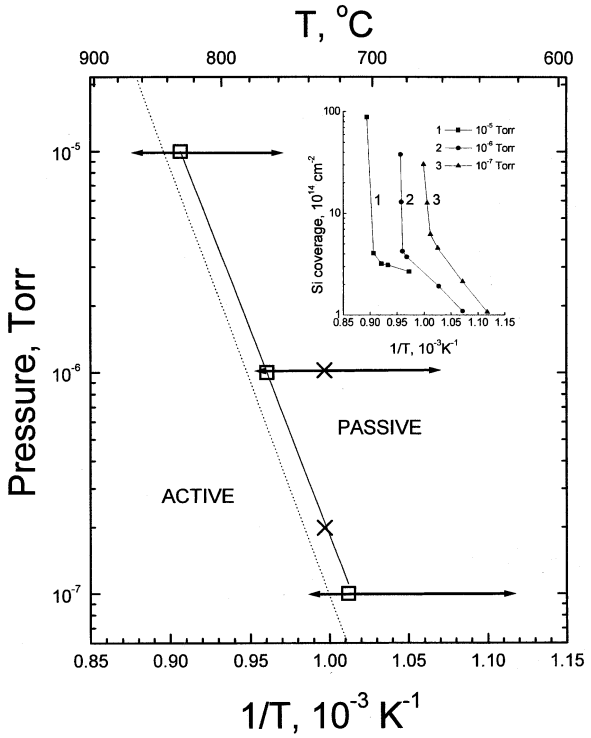

Fig. 2. The phase diagram for Si oxidation (solid line). The arrows show the temperature range covered in our experiments for each pressure. Dashed line: extrapolation of the experimental boundary curve of Smith and Ghidini3 (originally obtained for pressures in the range between 5×10^{-5} and 5×10^{-2} Torr). The inset shows the Si coverage on the Ag foil (proportional to the yield of SiO) as a function of the Si sample temperature for pressures of 10^{-7}, 10^{-6} and 10^{-5} Torr.

on Si substrate temperature is presented in the inset in Fig. 1. Because of the low SiO yield during the initial stages of passive oxidation at lower temperatures, data were accumulated during multiple runs of the experiment performed under identical conditions. At some temperature a steplike increase in the amount of SiO yield occurs. This temperature is thought to be the temperature of the transition from passive to active oxidation at the specified pressure. After oxidation at only several degrees above the transition temperature, a relatively sharp spot of SiO_x deposited on the Ag plate could be observed by the naked eye. The data obtained from the analogous measurements for different pressures (inset, Fig. 2) have been used to plot the phase diagram for silicon oxidation (Fig. 2). The phase diagram agrees well with an extrapolation of the phase diagram measured by Smith and Ghidini[3] at higher pressures and temperatures. Actually the processes of oxide film growth and etching are kinetically limited. When oxidation starts on a clean Si surface, SiO etching can occur at a measurable rate for $T > 600$°C during the initial stages of the process.[24] We observed some SiO desorption during the initial stages of oxidation as low as 100°C below the transition temperature. If the oxygen uptake (pressure) is large enough, the nucleation of oxide islands and eventually the growth of an oxide film occur. In other words, the phase diagram should depend on time (or initial surface coverage), as noted before. For oxidation in the passive regime, no detectable change in the integrated Si 2s peak intensity was observed after the initial 10 min of oxidation, which means that SiO desorption from the Si sample during passive oxidation occurs mainly during the initial stages of oxidation, in agreement with previous studies.[19] This fact allows us to conclude that SiO formation and transport into the gas phase does not play a significant role in oxide film growth.[42] However, we have carried out special measurements (described below) to determine if SiO transport into the gas phase takes place after the surface is completely covered by a continuous SiO_2 layer.

The most interesting region in the phase diagram in this study is the vicinity of the boundary on the low temperature – high pressure (passive oxidation) side. Here we want to find if (and how much) SiO generation and transport into the gas phase results, especially after the formation of a thin SiO_2 layer is complete and no clean Si surface remains exposed. A working hypothesis is that since (i) O_2 is not directly involved in the SiO_2 decomposition reaction ($Si + SiO_2 \rightarrow 2SiO$), and (ii) the reaction is observed under ultrahigh vacuum thermal annealing conditions, some SiO desorption should also take place during the growth of the oxide film. On the other hand, only the final fast stage of oxide film decomposition (conditions which are not relevant for "true" passive oxidation) has been studied in most previous experiments.

There exists little direct information about the rate of oxide decomposition and transport of SiO into the gas phase during the initial stage of vacuum decomposition before void formation; the reaction rates are too slow to be measured by conventional techniques. It is, however, important to know these rates

in order to compare them with the oxide growth rate and to better understand the possible role and extent of decomposition during film growth. Some insight into this problem can probably be provided by a study of the transition from the etching to the oxide growth regimes both in P–T space and in time, because the gaseous product of SiO_2 decomposition in the passive mode can most easily be observed in the vicinity of the transition point. Walkup and Raider[45] measured the desorption of SiO molecules in the gas phase at a fixed temperature in the range of 800–1200°C as a function of the O_2 flow rate. They observed a drop of SiO production upon transition through a critical flow rate to a level below their sensitivity limit ($\sim 3 \times 10^{-5}$ ML/s) within a few seconds. Engstrom *et al.*[24] examined the kinetics of the transition from active to passive oxidation by simultaneously monitoring the oxygen adsorbed on silicon by XPS and the gaseous SiO production using a mass spectrometer. Their results demonstrate a linear decrease in the SiO desorption rate with oxygen coverage for low coverage, which implies that the desorption rate is proportional to the Si surface area free of oxygen. The desorption reaction is strongly suppressed when the amount of adsorbed oxygen exceeds a critical value (2–4 ML, depending on temperature). The analysis of SiO wave forms in the MMBRS experiments[15] suggests that the rate constant for SiO desorption does not change with oxygen coverage, although the desorption rate decreases. These results are consistent with an inhomogeneous growth of the oxide film via oxide island nucleation and lateral growth with a competition between oxide growth and etching. The detectable SiO desorption in this regime occurs only on the clean Si surface and drops when the area covered by the oxide increases.

In Fig. 3 we present XPS spectra for Si that desorbs (via SiO) from the Si sample and becomes trapped on the Ag plate during: (a) oxide film thermal decomposition in vacuum, $P = 5 \times 10^{-10}$ Torr, $T = 730$°C, (b) decomposition under oxygen-deficient conditions, $P = 2 \times 10^{-7}$ Torr, $T = 730$°C, and (c) Si oxidation in the passive oxidation regime, $P = 10^{-6}$ Torr, $T = 730$°C. The oxidation conditions for (b) and (c) in the P–T space are shown as crosses in Fig. 2. Note that the conditions in (b) correspond to the boundary region between the passive and active oxidation regions. To measure the yields of SiO desorbing from the Si sample

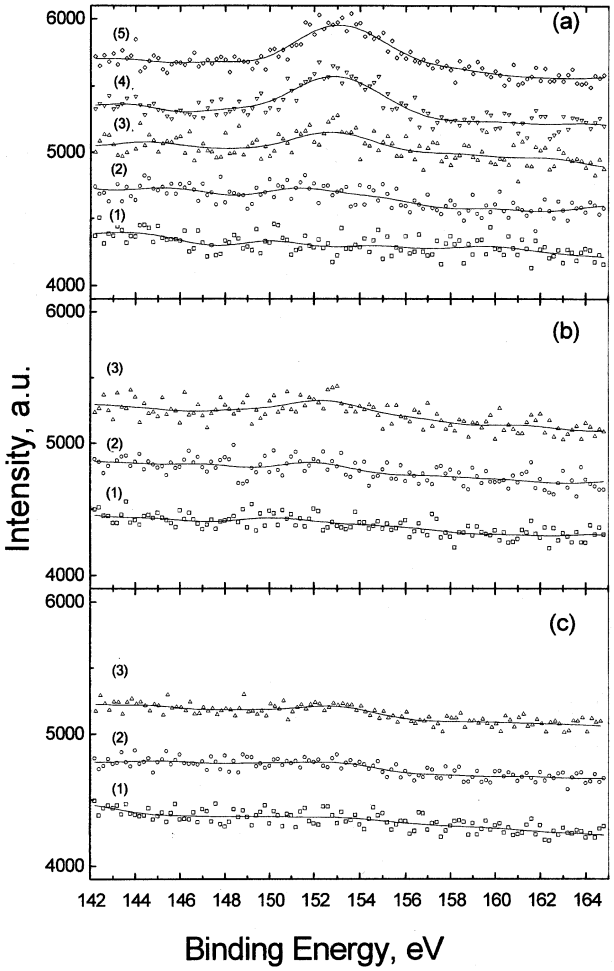

Fig. 3. XPS spectra for Si deposited on the Ag foil at 730°C under conditions of: (a) residual gas pressure of 5×10^{-10} Torr, deposition time (1) 15 min, (2) 20 min, (3) 25 min, (4) 30 min, (5) 60 min; (b) O_2 pressure of 2×10^{-7} Torr, deposition time (1) 1 h, (2) 2 h, (3) 3 h; and (c) O_2 pressure of 10^{-6} Torr, deposition time (1) 30 min, (2) 3 h, (3) 4 h. Both the raw data and a smoothed curve obtained by a fast Fourier transform filter are shown. The P–T conditions for (b) and (c) are shown in Fig. 2 as crosses.

entirely covered by the thin oxide film, we positioned the Ag foil in front of the Si sample *after* its oxidation at 715°C and 10^{-6} Torr for 20 min. According to the literature,[43] the thickness of the film is about ~ 7 Å under these oxidation conditions. The continuity of the oxide film is confirmed by its subsequent vacuum decomposition at 730°C [Fig. 3(a)]. No SiO yield into the gas phase was detected during the first 20 min after cutting off the oxygen supply. We found that the oxide decomposes entirely

during the following 10 min. This result confirms that decomposition occurs through void formation and growth, and a latent annealing time prior to rapid decomposition is needed for the nucleation and growth of voids to a size and a number sufficient to be measured.[26,28–30,32] The total amount of Si deposited on the Ag foil during vacuum annealing corresponds to 1.5–2 ML oxygen coverage on the Si sample prior to decomposition. For passive oxidation [Fig. 3(c)] there is no visible Si signal after the first 30 min of SiO accumulation on the foil (first 50 min of oxidation), but after 3–4 h of oxidation a small Si 2s peak clearly appears. The mean desorption rate determined as the total amount of Si trapped on the foil divided by the time of its accumulation is estimated to be about 1–3 $\times 10^{-5}$ ML/s from the integrated Si 2s peak intensity. The reduction of the oxygen pressure to $P = 2 \times 10^{-7}$ Torr at the same temperature [Fig. 3(b)] does not significantly increase the rate of SiO desorption. Though the peak signal to noise ratio is too small for one to make any conclusion about the kinetics of desorption, it seems that an accelerated desorption rate, typical for void formation and growth, is not observed. This is consistent with a very strong suppression of void formation even with very low partial pressures of oxygen.[26] This means that in the process of passive oxidation at higher pressures, at least at moderate or lower temperatures, a low fraction of oxygen incident on the film could be sufficient to suppress void formation and significant oxide desorption. But Fig. 3(c) shows quite clearly that a small yield of SiO into the gaseous phase can still take place even during passive oxidation. It is unclear at present if SiO originates heterogeneously (on defects) or homogeneously at the interface, and what reaction (SiO_2 decomposition or Si oxidation) results in the SiO formation. The results obtained from earlier studies of SiO_2 decomposition through void formation[26,28–30,32] (highly inhomogeneous lateral distribution of voids, the presence of only a few void sizes, void density increasing after intentional introduction of metal impurities, etc.) demonstrate that void nucleation occurs predominantly on defect sites which already exist prior to annealing. These can also be centers for decomposition during growth of the oxide film. Positron decay studies[23,32] show evidence for the presence of microvoids in thermal oxides, providing a further argument for the plausibility of SiO formation at the SiO_2/Si interface during the oxide film growth at high temperatures. These could be stable (at high temperatures) gaseous species trapped in voids in the film.

4. Summary

We have measured the total yield and mean rate of SiO desorption that occurs during both passive and active oxidation, and vacuum annealing of very thin oxide films ($\leq$ 7 Å). The total amount of Si desorbed during oxidation or annealing, and accumulated with high efficiency on a Ag plate placed in front of the Si sample, was measured using XPS. The results obtained give direct evidence that SiO formation and out-diffusion into the gas phase can occur during passive oxidation (we observed it at temperatures of ~ 700°C and under pressure of $\sim 10^{-6}$ Torr for a $\sim$ 7-Å-thick oxide film), though the rate of SiO desorption is estimated to be very low under these conditions, i.e. $\sim 10^{-5}$ ML/s. The thermal SiO_2 film decomposition can be quenched by very low partial pressures of O_2 in the gas phase. We also plotted the P–T phase diagram for silicon oxidation from our measurements in the pressure and temperature ranges of 10^{-7}–10^{-5} Torr and 620–870°C, respectively. It was shown that an observable quantity of SiO desorbs into the gas phase during the initial stages of passive oxidation at $\sim$ 100°C lower than the transition temperature.

Acknowledgments

The authors would like to thank Dr. H. C. Lu for useful discussions, and acknowledge the support of this work from the NSF (DMR-9701748 and ECS-9530984) and SRC (451).

References

1. J. J. Lander and J. Morrison, *J. Appl. Phys.* **33**, 2089 (1962).
2. C. Gelain, A. Cassuto and P. Le Goff, *Oxid. Met.* **3**, 139 (1971).
3. F. W. Smith and G. Ghidini, *J. Electrochem. Soc.* **129**, 1300 (1982).
4. M. R. Baklanov, V. N. Kruchinin, S. M. Repinsky and A. A. Shklyaev, *React. Solids* **7**, 1 (1989).
5. J. Seiple and J. P. Pelz, *Phys. Rev. Lett.* **73**, 999 (1994).

6. F. M. Ross, J. M. Gibson and R. D. Twesten, *Surf. Sci.* **310**, 243 (1994).
7. A. A. Shklyaev and T. Suzuki, *Phys. Rev. Lett.* **75**, 272 (1995).
8. N. Cabrera and N. F. Mott, *Rep. Prog. Phys.* **12**, 148 (1948).
9. B. E. Deal and A. S. Grove, *J. Appl. Phys.* **36**, 3770 (1965).
10. K. R. Lawless, *Rep. Prog. Phys.* **37**, 231 (1974).
11. A. Atkinson, *Rev. Mod. Phys.* **57**, 437 (1985).
12. H. Z. Massoud, J. D. Plummer and E. A. Irene, *J. Electrochem. Soc.* **132**, 2693 (1985).
13. A. M. Stoneham, C. R. M. Grovenor and A. Cerezo, *Philos. Mag.* **B55**, 201 (1987).
14. C.-J. Han and C. R. Helms, *J. Electrochem. Soc.* **134**, 1297 (1987).
15. M. P. D'Evelyn, M. M. Nelson and T. Engel, *Surf. Sci.* **186**, 75 (1987).
16. *The Si–SiO_2 System*, ed. P. Balk (Elsevier, Amsterdam, 1988).
17. N. F. Mott, S. Rigo, F. Rochet and A. M. Stoneham, *Philos. Mag.* **B60**, 189 (1989).
18. J. M. Delarious, C. R. Helms, D. B. Kao and B. E. Deal, *Appl. Surf. Sci.* **39**, 89 (1989).
19. T. Engel, *Surf. Sci. Rep.* **18**, 91 (1993).
20. C. J. Sofield and A. M. Stoneham, *Semic. Sci. Technol.* **10**, 215 (1995).
21. E. P. Gusev, H. C. Lu, T. Gustafsson and E. Garfunkel, *Phys. Rev.* **B52**, 1759 (1995).
22. W. A. Tiller, *J. Electrochem. Soc.* **130**, 501 (1983).
23. *Fundamental Aspects of Ultrathin Dielectrics on Si-Based Devices*, eds. E. Garfunkel, E. Gusev and A. Vul' (Kluwer, Dordrecht/Boston/London, 1998).
24. J. R. Engstrom, D. J. Bonser, M. M. Nelson and T. Engel, *Surf. Sci.* **256**, 317 (1991).
25. A. Ishizaka and Y. Shiraki, *J. Electrochem. Soc.* **133**, 666 (1986).
26. G. W. Rubloff, K. Hofmann, M. Liehr and D. R. Young, *Phys. Rev. Lett.* **58**, 2379 (1987).
27. G. D. Wilk, Yi Wei, H. Edwards and R. M. Wallace, *Appl. Phys. Lett.* **70**, 2288 (1997).
28. R. Tromp, G. W. Rubloff, P. Balk, F. K. LeGoues and E. J. van Loenen, *Phys. Rev. Lett.* **55**, 2332 (1985).
29. M. Liehr, J. E. Lewis and G. W. Rubloff, *J. Vac. Sci. Technol.* **A5**, 1559 (1986).
30. M. Liehr, H. Dallaporta and J. E. Lewis, *Appl. Phys. Lett.* **53**, 589 (1988).
31. Y.-K. Sun, D. J. Bonser and T. Engel, *Phys. Rev.* **B43**, 14309 (1991).
32. G. W. Rubloff, *J. Vac. Sci. Technol.* **A8**, 1857 (1990).
33. Y. Kobayashi, Y. Shinoda and K. Sugii, *Jpn. J. Appl. Phys.* **29**, 1004 (1990).
34. K. E. Johnson and T. Engel, *Phys. Rev. Lett.* **69**, 339 (1992).
35. Y.-K. Sun, D. J. Bonser and T. Engel, *J. Vac. Sci. Technol.* **A10**, 2314 (1992).
36. Y. Kobayashi and K. Sugii, *J. Vac. Sci. Technol.* **A10**, 2308 (1992).
37. A. A. Shklyaev, M. Aono and T. Suzuki, *Phys. Rev.* **B54**, 10890 (1996).
38. A. Feltz, U. Memmert and R. J. Behm, *Surf. Sci.* **314**, 34 (1994).
39. J. Seiple and J. P. Pelz, *J. Vac. Sci. Tech.* **A13**, 772 (1995).
40. H. C. Lu, E. P. Gusev, E. Garfunkel and T. Gustafsson, *Surf. Sci.* **351**, 111 (1996).
41. B. Mohadjeri, M. R. Baklanov, E. Kondoh and K. Maex, *J. Appl. Phys.* **83**, 3614 (1998).
42. S. I. Raider, in *The Physics and Chemistry of SiO_2 and the Si–SiO_2 Interface*, eds. C. R. Helms and D. E. Deal (Plenum, New York, 1988), p. 35.
43. Y. Takakuwa, M. Nihei, T. Horie and N. Miyamoto, *J. Non-Crystalline Solids* **179**, 345 (1994).
44. Y. Takakuwa, M. Nihei and N. Miyamoto, *Appl. Surf. Sci.* **117/118**, 141 (1997).
45. R. E. Walkup and S. I. Raider, *Appl. Phys. Lett.* **53**, 888 (1988).
46. *Practical Surface Analysis by Auger and X-Ray Photoelectron Spectroscopy*, eds. D. Briggs and M. P. Seah (John Wiley & Sons, 1983).
47. S. Tanuma, C. J. Powell and D. R. Penn, *Surf. Interface Anal.* **11**, 577 (1988).
48. *The Handbook of Semiconductor Silicon Technology*, eds. W. C. O'Mara, R. B. Herring and L. P. Hunt (Noyes, Park Ridge, New Jersey, 1990).